Title: 125 characters

Evaluating the effectiveness of distortion self-correction for CEST-EPI

Jianpan Huang[1,2*], Se Weon Park[2,3], Kannie WY Chan[2-6*]

[1]Department of Diagnostic Radiology, The University of Hong Kong, Hong Kong, China
[2]Hong Kong Centre for Cerebro-Cardiovascular Health Engineering, Hong Kong, China
[3]Department of Biomedical Engineering, City University of Hong Kong, Hong Kong, China
[4]Russell H. Morgan Department of Radiology and Radiological Science, The Johns Hopkins University School of Medicine, Baltimore, MD, USA
[5]Tung Biomedical Sciences Centre, City University of Hong Kong, Hong Kong, China
[6]City University of Hong Kong Shenzhen Research Institute, Shenzhen, China

Synopsis: 100 words (combined 4 sections)

Motivation: EPI-based CEST (CEST-EPI) is fast but suffers from image distortion caused by field susceptibility.

Goal: We aimed to evaluate the effectiveness of using the field map generated by the Z-spectra to achieve the distortion self-correction (DISC) of for single-shot CEST-EPI without additional acquisition of a field map.

Approach: The effectiveness of DISC strategy was demonstrated in CEST-EPI experiments of a creatine phantom and in vivo mice. CEST-RARE was used as a reference.

Results: Without acquiring an additional field map, DISC retrospectively and effectively corrected geometric distortion in CEST-EPI, leading to improved SSIM and spatial CEST contrasts.

Impact: 40 words

We evaluated the effectiveness of using the field map generated by the Z-spectra to achieve the distortion self-correction for single-shot CEST-EPI. Results showed that DISC retrospectively and effectively corrected geometric distortion in CEST-EPI without acquiring an additional field map.

Body of the Abstract: 750 words (references not included)

Introduction

Chemical exchange saturation transfer (CEST) MRI is a promising molecular imaging technique that enables the detection of low-concentration molecules[1, 2]. Many readout sequences have been used for CEST acquisition, such as fast/turbo spin echo (FSE/TSE) or rapid acquisition with relaxation enhancement (RARE)[3-7] and echo planar imaging (EPI)[8-13]. FSE/TSE/RARE is a commonly used CEST acquisition sequence that can acquired images with good quality, but the scan time is relatively long. EPI is a fast acquisition alternative but suffers from image distortion caused by field susceptibility. Two commonly used EPI distortion correction methods are field-mapping method[14, 15] and the top-up method[8, 16]. Both methods require additional scans. In CEST imaging, the field map can be generated from Z-spectra by data interpolation and minimum search, and typically is used to correct Z-spectra[17]. Here, we evaluated the effectiveness of using the field map generated by the Z-spectra to achieve the distortion self-correction (DISC) of for single-shot CEST-EPI without additional acquisition of a field map. The effectiveness of DISC strategy was evaluated in creatine phantom and in vivo mouse brain experiments.

Methods

All MRI experiments were performed on a 3T Bruker BioSpec system. In phantom experiment, creatine tubes with different concentrations, i.e., 0mM, 5mM, 10mM, 20mM,30 mM, 40mM, and 50mM, were prepared by dissolving the creatine in deionized water titrated to pH 7.3. In animal experiment, six C57BL/6 male mice were used. CEST MRI sequence was a continuous-wave saturation module followed by EPI or RARE as a readout module. The MRI parameters were as follows: B_1=0.8 μT, t_{sat}=3s, TR=5s, TE=43ms, FOV=20×20mm^2, matrix size=96×96, bandwidth=250kHz (CEST-EPI), RARE factor=24 (CEST-RARE). For each CEST dataset, 73 CEST images at saturation offsets ranging from -20 to 20 ppm and three M_0 images at 200 ppm were acquired. The scan time of each CEST dataset was 6min20s for CEST-EPI and 25min20s for CEST-RARE. The DISC procedures for CEST-EPI are illustrated in Figure 1. Structural similarity index measure (SSIM) was used to assess the correction effectiveness of the geometric distortion.[18] The creatine CEST map of phantom was generated using magnetization transfer asymmetry (MTR_{asym}),[19] while the amide CEST and relayed nuclear Overhauser effect (rNOE) maps were generated using Lorentzian difference analysis.[20]

Results and Discussion

CEST-EPI images of the creatine phantom displayed obvious geometric distortion when compared to CEST-RARE image (Figure 1A-C). ΔB_0 map revealed that the distortion was primarily caused by B_0 inhomogeneity. The SSIM values for the entire CEST dataset and the creatine CEST map in CEST-EPI were 0.818 and 0.875, respectively. However, after applying the DISC, these two values were improved to 0.921 and 0.933, respectively, as clearly demonstrated by the results of DISC-CEST-EPI. Furthermore, the correlation results (Figure 2D-E) demonstrated that DISC-CEST-EPI (R^2 = 0.9682) exhibited better spatial consistency with CEST-RARE compared to CEST-EPI (R^2 = 0.9843). These findings suggested that the DISC strategy effectively corrects the geometric distortion in CEST-EPI.

CEST-EPI images of a mouse brain displayed significant geometric distortion, particularly at interfaces such as the brain-muscle and muscle-air interfaces (yellow arrows in Figure 3A). Regions with large B_0 inhomogeneity, as indicated by the green arrows in Figure 3B, were particularly affected by severe distortion. The distortion was also evident in the amide CEST and rNOE maps (Figure 3C-D). Notably, the application of distortion self-correction in DISC-CEST-EPI led to significant improvements in both the original CEST image (Figure 3A) and the CEST contrast maps (Figure 3C-D). The SSIM values for six mice (Table 1) demonstrated improved image quality in all tested cases. Specifically, DISC-CEST-EPI improved the SSIM value of the entire CEST dataset from 0.634±0.068 to 0.681±0.069. Moreover, the SSIM values of the amide CEST and rNOE maps increased from 0.909±0.014 and 0.894±0.010 to 0.940±0.012 and 0.929±0.007, respectively. Correlation analysis between CEST-EPI/DISC-CEST-EPI and CEST-RARE, using mean values of amide CEST and rNOE extracted from seven regions of interest in the mouse brain (Figure 4A), showed that DISC-CEST-EPI exhibited better spatial consistency with correlation coefficients of R=0.8867 and 0.9158, respectively (Figure 4B-C). These findings strongly supported the effectiveness of the DISC strategy in correcting geometric distortion for in vivo CEST MRI.

Conclusion

In this study, we evaluated the use of the field map generated by the Z-spectra for DISC of single-shot CEST-EPI. Our results, obtained from a creatine phantom and in vivo mouse brains, demonstrated that DISC effectively corrected geometric distortion in CEST-EPI, leading to improved SSIM and spatial CEST contrasts. Notably, DISC can be applied retrospectively to correct geometric distortion in CEST-EPI without an additional field map acquisition.

Acknowledgement

Authors would like to acknowledge the funding supports from The University of Hong Kong: 109000487, 204610401 and 204610519. Research Grants Council (11102218, 11200422, RFS2223-1S02, C1134-20G); City University of Hong Kong (7005433, 7005626, 9609307, 9610560 and 9610616), National Natural Science Foundation of China (81871409), Tung Biomedical Sciences Centre and Hong Kong Centre for Cerebro-cardiovascular Health Engineering.

REFERENCES

1. Van Zijl PC, Yadav NN. Chemical exchange saturation transfer (CEST): what is in a name and what isn't? *Magn Reson Med*. 2011;65(4):927-948.
2. Ward K, Aletras A, Balaban RS. A new class of contrast agents for MRI based on proton chemical exchange dependent saturation transfer (CEST). *J Magn Reson*. 2000;143(1):79-87.
3. Liu G, Ali MM, Yoo B, Griswold MA, Tkach JA, Pagel MD. PARACEST MRI with improved temporal resolution. *Magnetic Resonance in Medicine: An Official Journal of the International Society for Magnetic Resonance in Medicine*. 2009;61(2):399-408.
4. Jones CK, Schlosser MJ, Van Zijl PC, Pomper MG, Golay X, Zhou J. Amide proton transfer imaging of human brain tumors at 3T. *Magnetic Resonance in Medicine: An Official Journal of the International Society for Magnetic Resonance in Medicine*. 2006;56(3):585-592.
5. Zhou J, Blakeley JO, Hua J, et al. Practical data acquisition method for human brain tumor amide proton transfer (APT) imaging. *Magnetic Resonance in Medicine: An Official Journal of the International Society for Magnetic Resonance in Medicine*. 2008;60(4):842-849.
6. Huang J, Lai JH, Tse KH, et al. Deep neural network based CEST and AREX processing: Application in imaging a model of Alzheimer's disease at 3 T. *Magnetic Resonance in Medicine*. 2022;87(3):1529-1545.
7. Zhang Y, Yong X, Liu R, et al. Whole-brain chemical exchange saturation transfer imaging with optimized turbo spin echo readout. *Magnetic Resonance in Medicine*. 2020;84(3):1161-1172.
8. Akbey S, Ehses P, Stirnberg R, Zaiss M, Stöcker T. Whole-brain snapshot CEST imaging at 7 T using 3D-EPI. *Magnetic resonance in medicine*. 2019;82(5):1741-1752.
9. Huang J, Zhang M, Lu J, Cai C, Chen L, Cai S. A fast chemical exchange saturation transfer imaging scheme based on single-shot spatiotemporal encoding. *Magn Reson Med*. 2017;77(5):1786-1796.
10. Mueller S, Stirnberg R, Akbey S, et al. Whole brain snapshot CEST at 3T using 3D-EPI: Aiming for speed, volume, and homogeneity. *Magn Reson Med*. 2020;84(5):2469-2483.
11. Sun PZ, Benner T, Kumar A, Sorensen AG. Investigation of optimizing and translating pH-sensitive pulsed-chemical exchange saturation transfer (CEST) imaging to a 3T clinical scanner. *Magn Reson Med*. 2008;60(4):834-841.
12. Zhou J, Lal B, Wilson DA, Laterra J, Van Zijl PC. Amide proton transfer (APT) contrast for imaging of brain tumors. *Magnetic Resonance in Medicine: An Official Journal of the International Society for Magnetic Resonance in Medicine*. 2003;50(6):1120-1126.
13. Zu Z, Janve VA, Xu J, Does MD, Gore JC, Gochberg DF. A new method for detecting exchanging amide protons using chemical exchange rotation transfer. *Magnetic Resonance in Medicine*. 2013;69(3):637-647.
14. Jezzard P, Balaban RS. Correction for geometric distortion in echo planar images from B0 field variations. *Magnetic resonance in medicine*. 1995;34(1):65-73.
15. Poblador Rodriguez E, Moser P, Dymerska B, et al. A comparison of static and dynamicΔ B0 mapping methods for correction of CEST MRI in the presence of temporal B0 field variations. *Magn Reson Med*. 2019;82(2):633-646.
16. Andersson JL, Skare S, Ashburner J. How to correct susceptibility distortions in spin-echo echo-planar images: application to diffusion tensor imaging. *Neuroimage*. 2003;20(2):870-888.
17. Kim M, Gillen J, Landman BA, Zhou J, Van Zijl PC. Water saturation shift referencing (WASSR) for chemical exchange saturation transfer (CEST) experiments. *Magn Reson Med*. 2009;61(6):1441-1450.
18. Wang Z, Bovik AC, Sheikh HR, Simoncelli EP. Image quality assessment: from error visibility to structural similarity. *IEEE transactions on image processing*. 2004;13(4):600-612.

19. Zhou J, Zaiss M, Knutsson L, et al. Review and consensus recommendations on clinical APT-weighted imaging approaches at 3T: Application to brain tumors. *Magn Reson Med*. 2022;
20. Jones CK, Polders D, Hua J, et al. In vivo three-dimensional whole-brain pulsed steady-state chemical exchange saturation transfer at 7 T. *Magnetic resonance in medicine*. 2012;67(6):1579-1589.

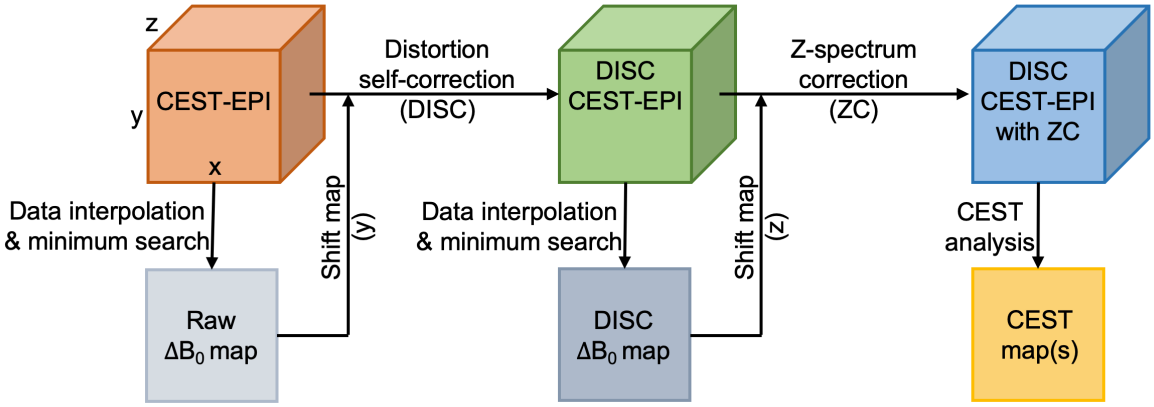

FIGURE 1 *Schematic diagram of the distortion self-correction (DISC) flow for single-shot CEST-EPI*. First, the ΔB_0 map was generated from CEST-EPI and converted into pixel shift map. Second, the pixel shift map was used to correct geometric distortion by interpolating and shifting the signal intensity of each PE line to generate DISC-CEST-EPI dataset. Finally, the DISC ΔB_0 map was generated from the DISC-CEST-EPI dataset and used for Z-spectrum correction (ZC). Frequency encoding is along x axis, phase encoding is along y axis.

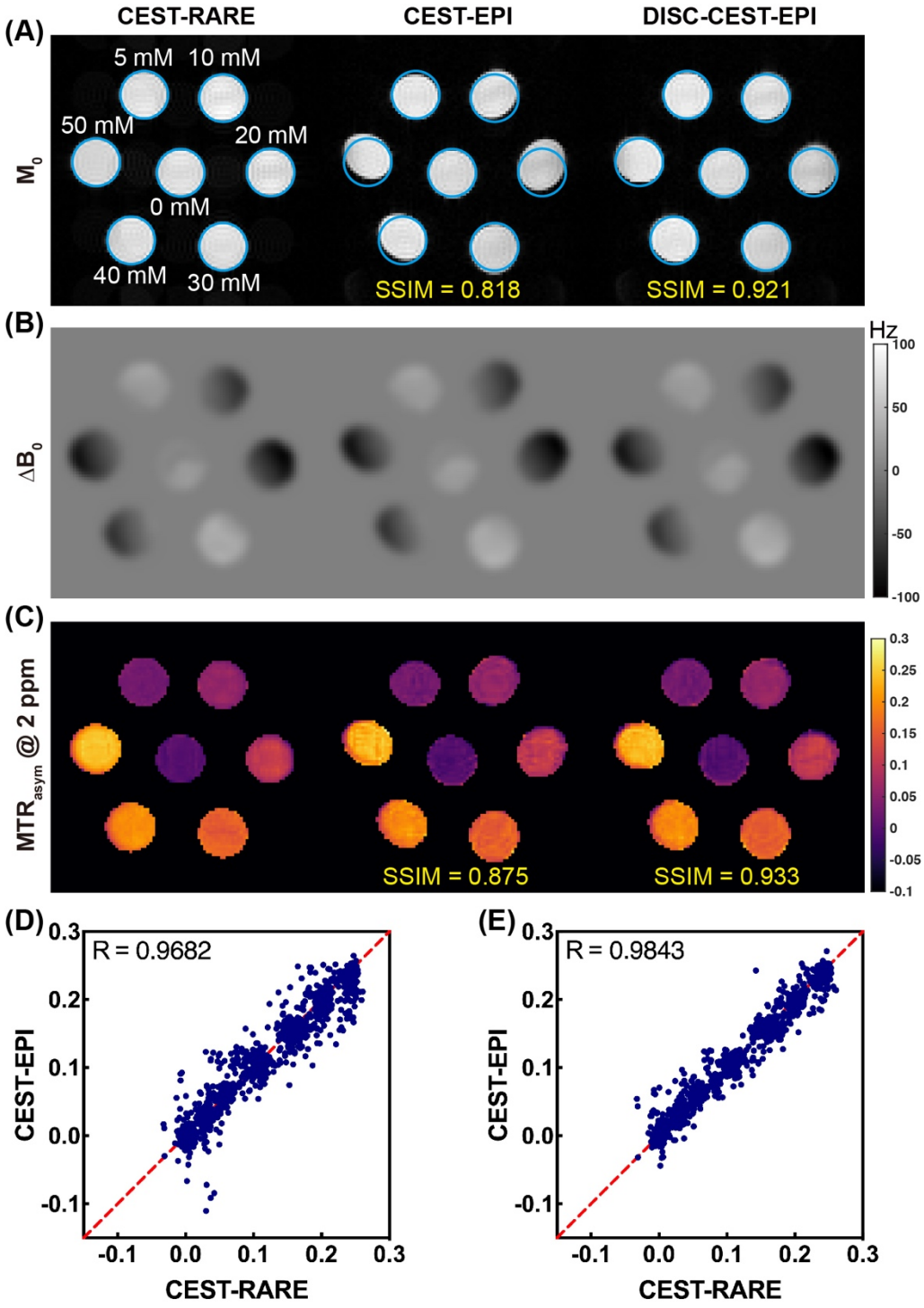

FIGURE 2 *Comparison of CEST-RARE with CEST-EPI/DISC-CEST-EPI in a creatine phantom.* (A) Original CEST images (M_0 images). (B) ΔB_0 maps. (C) Creatine CEST maps. (D) Spatial correlation of creatine CEST values between CEST-RARE and CEST-EPI/DISC-CEST-EPI.

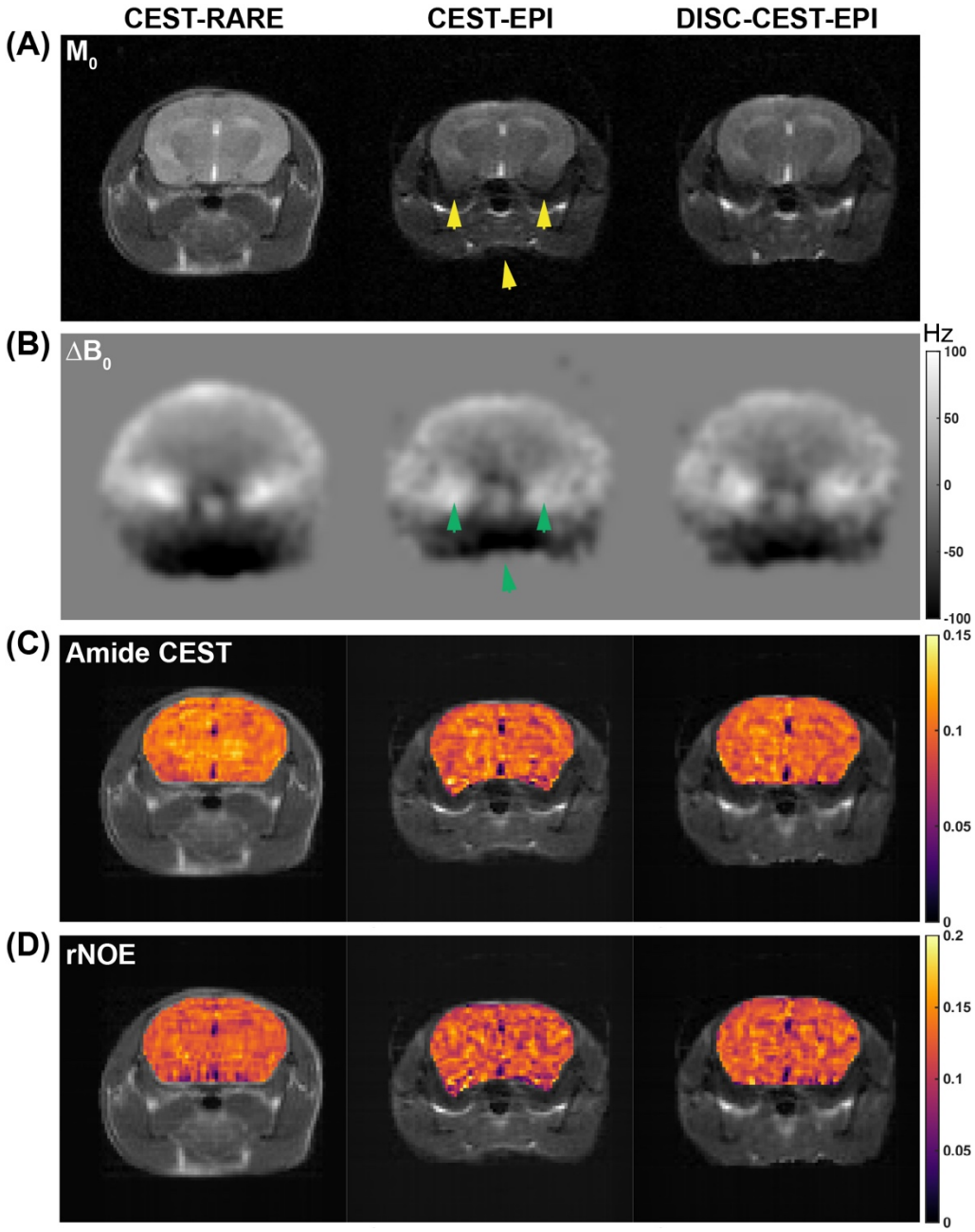

FIGURE 3 *Comparison of CEST-RARE with CEST-EPI/DISC-CEST-EPI in an in vivo mouse brain.* (A) Original CEST images (M_0 images). (B) ΔB_0 maps. (C) Amide CEST maps. (D) rNOE maps.

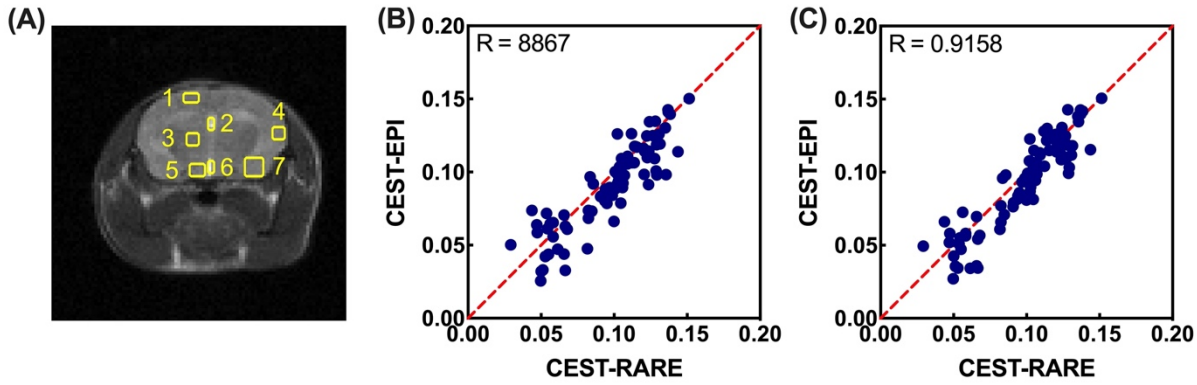

FIGURE 4 Spatial correlation of CEST values, including amide CEST and rNOE contrasts, between CEST-RARE and CEST-EPI/DISC-CEST-EPI. (A) Seven regions of interest in the mouse brain were selected for correlation analysis. (B) Correlation of CEST-RARE with CEST-EPI. (C) Correlation of CEST-RARE with DISC-CEST-EPI.

TABLE 1 Comparison of SSIM values for CEST-EPI and DISC-CEST-EPI in all mice.

Mouse No.	All CEST images		APT map		rNOE map	
	CEST-EPI	DISC-CEST-EPI	CEST-EPI	DISC-CEST-EPI	CEST-EPI	DISC-CEST-EPI
1	0.515	0.562	0.883	0.916	0.888	0.925
2	0.624	0.682	0.909	0.943	0.878	0.919
3	0.636	0.689	0.921	0.949	0.901	0.931
4	0.63	0.666	0.92	0.945	0.891	0.925
5	0.712	0.769	0.908	0.946	0.904	0.941
6	0.688	0.717	0.913	0.938	0.902	0.93
Mean	0.634	0.681	0.909	0.940	0.894	0.929
SD	0.068	0.069	0.014	0.012	0.010	0.007
P value	0.0002 ***		<0.0001 ****		<0.0001 ****	